

# Improving performance of InGaN LEDs on sapphire substrates

**Mike Cooke** reports on research into semipolar growth, quantum well barrier composition and zinc oxide enhancements.

**C**ommercial indium gallium nitride (InGaN) light-emitting diodes (LEDs) are mostly produced on sapphire substrates, balancing cost versus performance.

Cost can be reduced further by growing III-nitride materials on silicon, but maintaining adequate performance is challenging due to a larger lattice mismatch that generates a higher density of crystal defects.

In the other direction, there are more expensive substrate materials — e.g. silicon carbide and gallium nitride — with smaller lattice mismatches generating higher-quality crystal structures. Further, GaN substrates can be cut in non-standard crystal orientations that allow higher performance LEDs to be created.

Here we report on some recent research work that attempts to improve the performance of LEDs grown on sapphire. This work includes techniques that attempt to implement non-standard crystal orientations, modifying the standard multiple quantum well (MQW) structure, and combining GaN and zinc oxide (ZnO).

## Semipolar growth

Two research groups have reported the growth of semipolar-oriented III-nitride on sapphire, promising more efficient LEDs at reduced cost. Semipolar GaN substrates are typically restricted to very expensive 10mm x 10mm pieces of free-standing or bulk material. Growth of semipolar GaN on sapphire results in low crystal quality in general.

Semipolar devices are attractive for longer wavelengths because electric charge polarization of the GaN chemical bond results in large polarization electric fields that inhibit electron-hole recombination to photons in the MQWs, reducing efficiency in conventional c-plane LEDs. This is often referred to in the literature as the quantum-confined Stark effect (QCSE).

Growth of devices in semipolar or nonpolar directions reduces the polarization electric field and reduces the quantum efficiency decrease, efficiency droop, and the

green and yellow gaps in wavelength coverage associated with QCSEs.

Another advantage of semipolar material is improved incorporation of indium in InGaN layers. High-indium-content InGaN tends to decompose, with indium evaporation, or to segregate into regions of varying compositions, leading to localized states.

## Triangular nanostructures

In one piece of work producing semipolar III-nitride material on sapphire, University of New Mexico (UNM), USA, fabricated triangular-nanostructure core-shell LEDs (TLEDs, Figure 1) on c-plane substrates [Ashwin K. Rishinaramangalam et al, Appl. Phys. Express, vol9, p032101, 2016]. The performance results are described as "preliminary".

The researchers comment: "Upon optimization of these TLEDs to being on par with existing technologies on free-standing GaN, the low cost associated with this approach could potentially become the driving force towards commercial adoption."

By using triangular nanostructures with semipolar sidewalls, the UNM researchers hope to access the advantages for light emission without the non-commercial costs of free-standing substrates.

The researchers prepared a 2µm n-GaN on sapphire template using metal-organic chemical vapor deposition (MOCVD). A 120nm silicon nitride layer was patterned into micron-scale stripes using interferometric lithography. The silicon nitride dielectric also functioned as electrical insulation in the resulting devices. A second lithography step was used to define the device and contact regions. The exposed regions of the silicon nitride were dry etched and the wafer surface cleaned using a 'piranha solution' process before nanostructure growth.

The new growth was carried out with continuous-flow MOCVD. The core was silicon-doped n-GaN. The fast growth of the c-plane leads to emergence of a triangular cross-section with semipolar (10 $\bar{1}$ 1) plane sides.

The researchers then applied a thin n-type aluminium gallium nitride (AlGaN) layer to block reverse leakage currents, to getter oxygen impurities, and to fill defects in the silicon nitride mask/insulation.

Further growth consisted of n-GaN electron injection, four InGaN quantum wells (QWs) in GaN barriers (3nm/9nm), and finally a p-GaN contact. The c-plane surfaces on the apex of the triangular cross-section re-emerged during p-GaN growth. The researchers attribute this to the use of hydrogen-rich growth conditions and the faster growth ( $\sim 3\times$ ) of p-GaN on the  $(10\bar{1}1)$  plane, compared with c-plane.

LEDs were fabricated with indium tin oxide (ITO) transparent conducting current-spreading layer, titanium/aluminium/nickel/gold n-electrode, and titanium/gold n- and p-contact pads.

The devices were tested under pulsed currents ( $2\mu\text{s}$ , 2% duty cycle). The electroluminescence (EL) was broadband and significant wavelength blue-shift was seen with increasing current (Figure 2). Wavelength shifts with semipolar devices are usually much smaller than those of c-plane LEDs. Since the peak was to one side of the broadband of emitted radiation, the researchers used the dominant wavelength to characterize the shift. At  $50\text{A}/\text{cm}^2$  current density, the dominant wavelength was  $\sim 465\text{nm}$  compared with a peak at  $\sim 425\text{nm}$ .

Electron microscope analysis showed the quantum well thicknesses to be non-uniform, thus explaining the broadband emission. The wells were thicker near the apex of the triangular cross-section. The researchers also believe that long-range variation in indium composition of the quantum wells played a role in the broad-

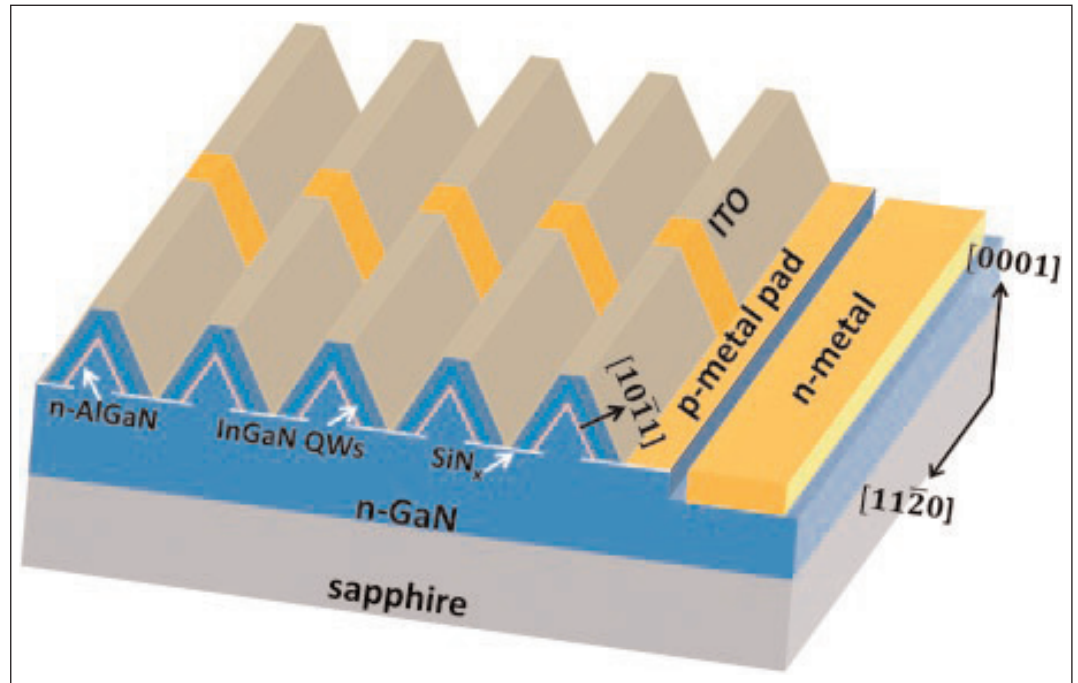


**Figure 1. Illustration of section of triangular-stripe core-shell nanostructure LED.**

band nature of the spectra. Energy dispersive x-ray spectroscopy revealed indium composition 1.5x higher nearer the apex compared with the sidewall.

The researchers explain: "For low injection currents, the path of least resistance is through the thick, high-indium-content QWs near the apex. This results in longer-wavelength emission ( $\sim 480\text{nm}$ ) at low current density, primarily from the QWs near the

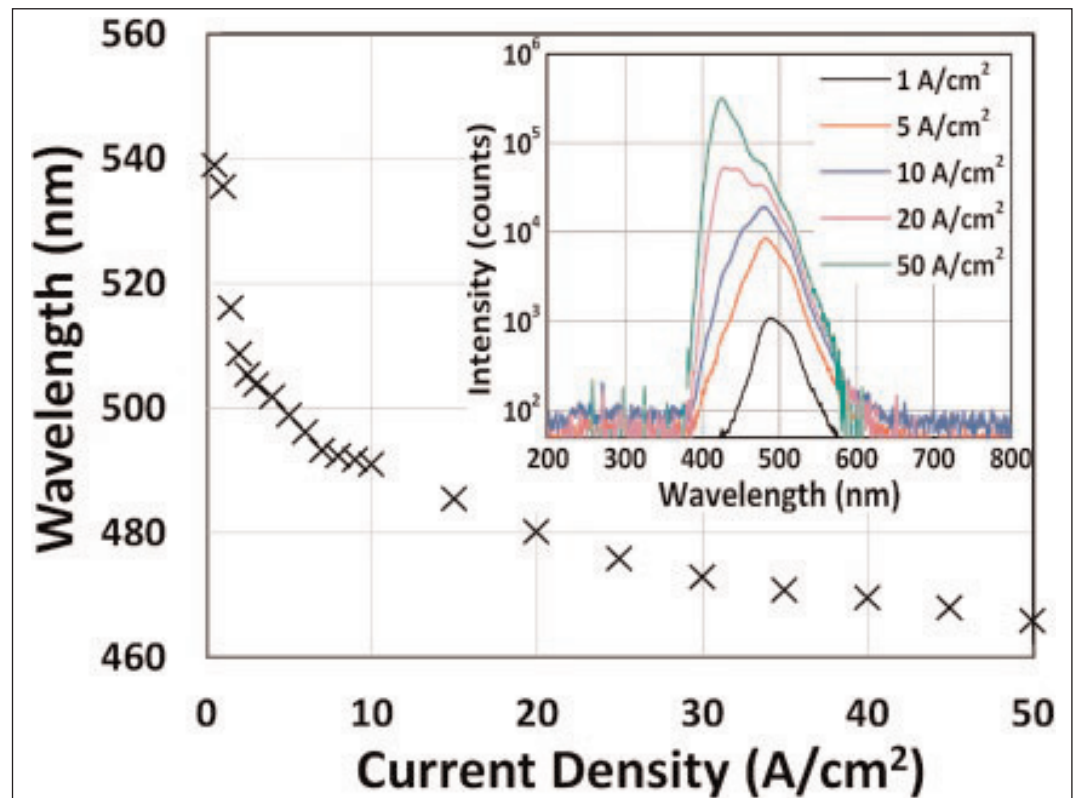


**Figure 2. EL dominant wavelength as function of current density. Inset shows EL spectra.**

apexes. As the current density is increased, the current spreading across the nanostructure is improved and a short-wavelength EL peak near 425nm emerges. This peak is attributed to the thin, low-indium-content QWs on the main sidewalls of the triangular stripe. The peak near 425nm shows very small shift in wavelength as a function of current density, as expected for uniform semipolar QWs."

### Overgrowth

University of Sheffield in the UK has also developed semipolar GaN/sapphire, demonstrating its use in long-wavelength InGaN single quantum well (SQW) LEDs [J. Bai et al, Appl. Phys. Lett., vol107, p261103, 2015]. Green to amber devices with peak wavelengths as long as 600nm at 100mA were produced. The researchers describe the EL as "strong" at 100mA.

The Sheffield research developed an overgrowth technique for production of (11 $\bar{2}$ 2) GaN on m-plane sapphire. The team sees applications for solid-state lighting and opto-genetics. Yellow light is particularly useful for controlling the activity of genetically modified cells such as neurons.

The Sheffield group notes that previous semipolar GaN on sapphire devices have been limited to blue and green wavelengths. The researchers comment: "Demonstration of yellow or even longer wavelength such as amber semipolar LEDs with device performance grown on foreign substrates has not yet been reported, as further improvement in growth technologies including crystal quality and enhancing indium incorporation into GaN is requested."

A single layer of (11 $\bar{2}$ 2) GaN was grown by MOCVD on m-plane sapphire using an aluminium nitride (AlN) buffer. The GaN layer was patterned into microrods using photolithographic techniques (Figure 3). The silicon dioxide used as mask was left on top of the GaN microrods.

More MOCVD is then carried out to give an overgrowth (11 $\bar{2}$ 2) GaN template layer about 4 $\mu$ m thick. The silicon dioxide blocks and coalesces defects, reducing dislocation densities to the range 1–4 $\times$ 10<sup>8</sup>/cm<sup>2</sup> and basal stacking fault densities to 1–4 $\times$ 10<sup>4</sup>/cm. X-ray diffraction (XRD) analysis suggests that the process results in a crystal quality approaching that for c-plane GaN on sapphire used for growth of ultra-high bright-

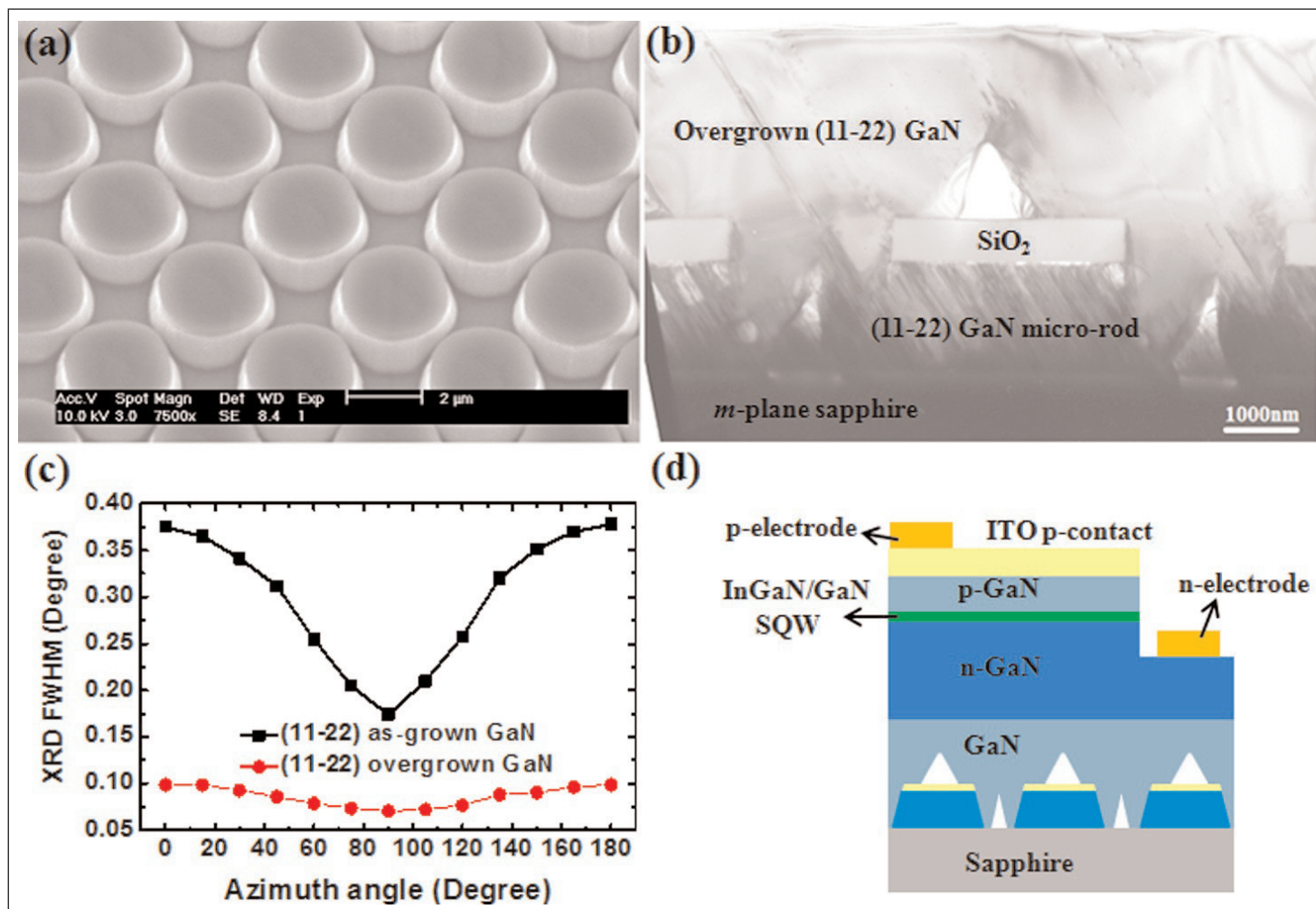
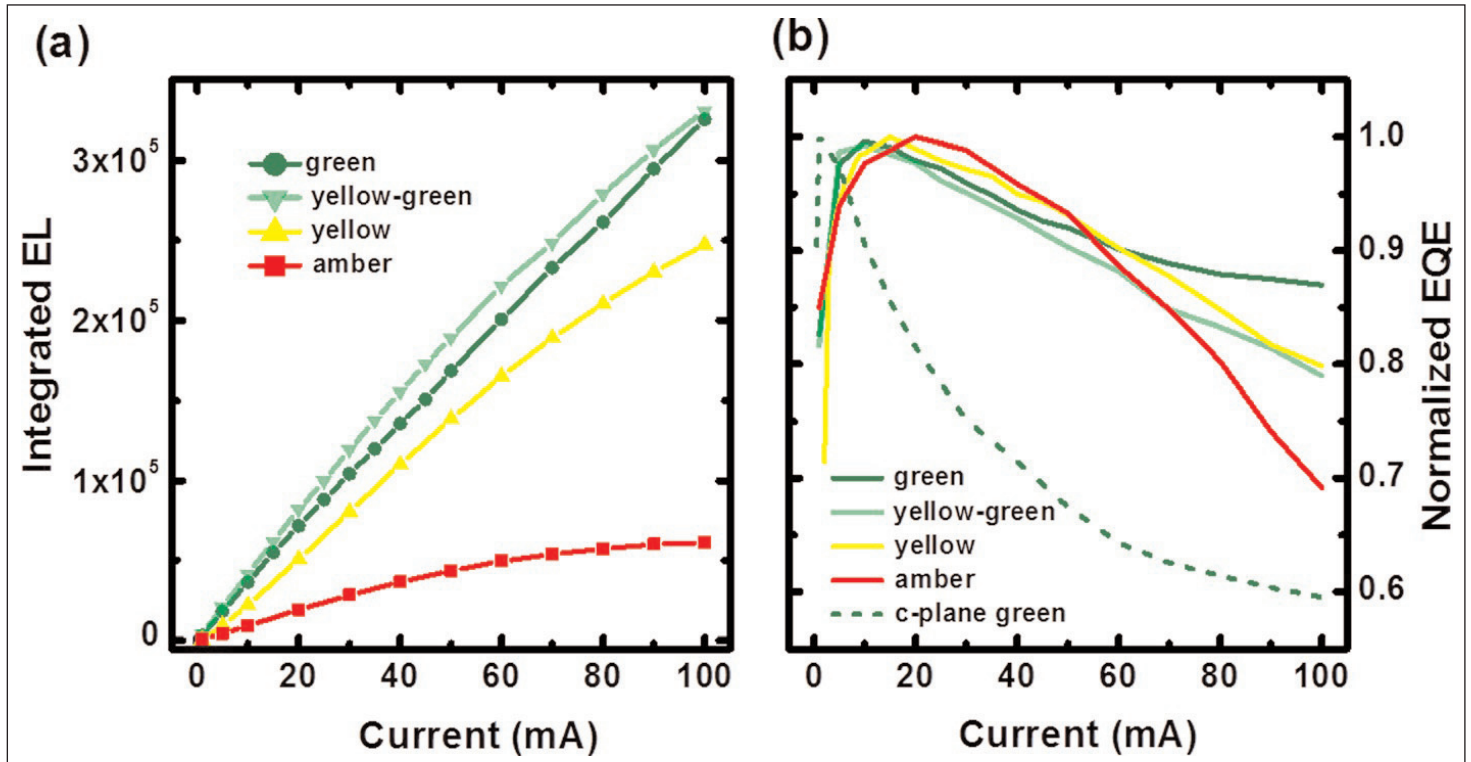


Figure 3. (a) SEM image of micro-rod GaN template; (b) TEM image of (11 $\bar{2}$ 2) GaN overgrown on microrods; (c) XRD full-widths at half maximum (FWHMs) of overgrown (11 $\bar{2}$ 2) GaN and (11 $\bar{2}$ 2) GaN template, measured at azimuth angles ranging from 0° to 180°; (d) schematic of (11 $\bar{2}$ 2) InGaN SQW LED.



**Figure 4. Light output (a) and normalized EQE (b) of the four LEDs as function of current from 1mA to 100mA. Commercial c-plane green LED (dashed line) reference.**

ness blue LEDs.

InGaN SQW structures were grown on the templates. The n-GaN and p-GaN layers were 1 $\mu$ m and 150nm, respectively. Lateral LEDs on 0.33mm x 0.33mm mesas were fabricated with 100nm indium tin oxide transparent conducting p-contact. The n-contact consisted of titanium/aluminium/titanium/gold. The contact pads were titanium/gold.

LEDs with four different color spectra were produced: green, green-yellow, yellow, and amber. As the wavelength of the light increases, the peaks become broader. In the case of the amber LED, the 600nm peak has a shoulder centered on 630nm at 100mA injection. The researchers say that this behavior is indicative of increasing indium separation at the higher compositions needed for longer wavelengths.

The peak wavelength underwent a blue-shift to shorter wavelengths with increasing current. The amount of shift was greatest with the longer-wavelength devices with high indium content. The green, green-yellow and yellow LEDs shifted 8nm, 15nm, and 19nm, respectively, between 1mA and 100mA. In c-plane green LEDs the corresponding shift is typically 13nm.

The researchers comment: "This suggests that the QCSEs in our (11 $\bar{2}2$ ) LEDs are effectively suppressed."

The amber devices had an even greater shift that could indicate significant segregation effects with lower-energy localized states being populated at low current injection. These states fill up at higher currents forcing shorter-wavelength transitions, accounting for the large  $\sim$ 50nm shift. In fact, in the lower current

injection range less than 20mA one could consider the LED to be emitting red light (620–740nm).

Problems with fabrication also increased the turn-on voltage of the amber devices ( $\sim$ 4V at 20mA). In particular, the p-GaN layer had to be grown at a lower temperature than normal to avoid damage to the InGaN single quantum well. The 20mA voltage for the other devices was in the range 3.0–3.4V, which is standard for InGaN LEDs.

The amber device also suffers from lower light output (Figure 4). All devices have better external quantum efficiency (EQE) performance in terms of droop, compared with commercial c-plane devices. The EQEs at 100mA relative to the maximum were 87%, 80%, 79% and 69% for the corresponding green, green-yellow, yellow and amber devices. The conventional c-plane device in the figure had an EQE at 49% of the maximum ( $\sim$ 3mA).

### Barrier enhancement

South China University of Technology has shown improved power and efficiency performance for InGaN LEDs with 1.2% indium-content multiple-quantum-well (MQW) barriers [Zhiting Lin et al, J. Phys. D: Appl. Phys., vol49, p115112, 2016].

The purpose of the research was to study the effect of indium in MQW barriers. Most commercial MQW designs use pure GaN barriers (i.e. 0% indium).

The epitaxial heterostructures were grown by MOCVD on 2-inch (0001) patterned sapphire (Figure 5). The undoped buffer layer was 4 $\mu$ m. The n-GaN contact was

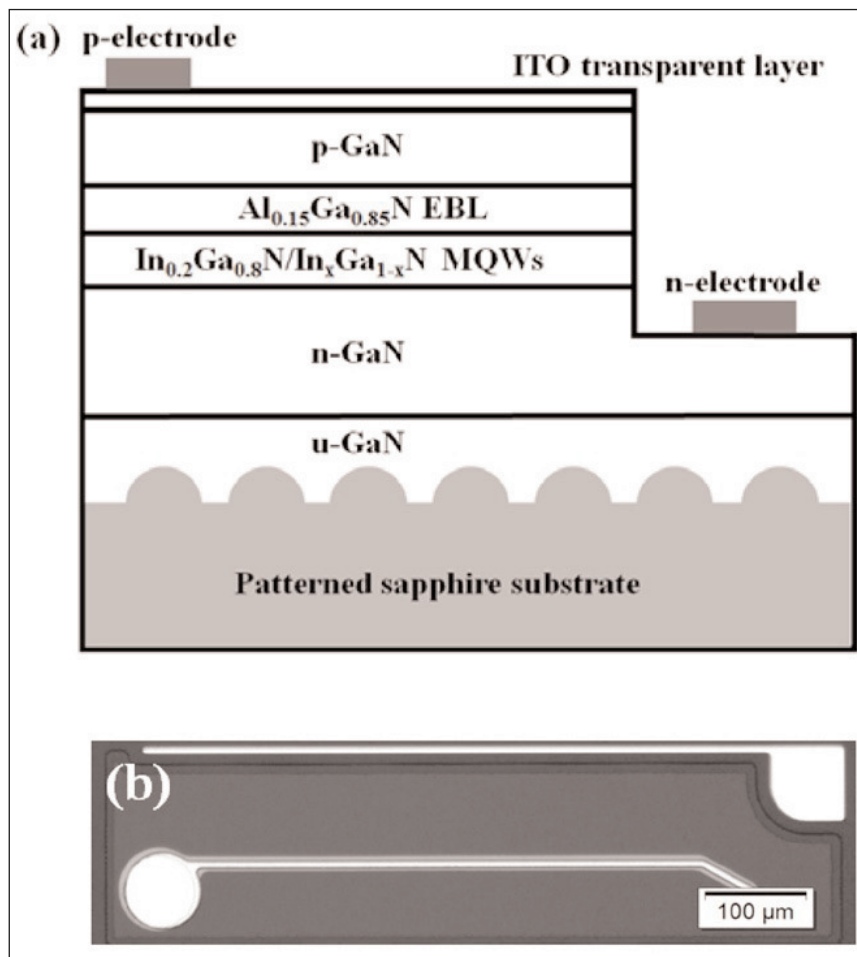


**Figure 5. (a) Epitaxial structure of as-grown LEDs; (b) optical micrograph of chip.**

3  $\mu\text{m}$ . The electron-blocking layer (EBL) and p-contact were 20nm and 150nm, respectively.

The MQW region consisted of seven 3nm wells separated by 14nm barriers. The wells had 20% indium content. The variation in indium content in the barriers was achieved through changing the trimethyl-indium

precursor flux. The indium content was evaluated using XRD analysis.

Standard InGaN LED chips were fabricated with 250nm indium tin oxide (ITO) transparent conductor, and chromium/platinum/gold n- and p-electrodes. The chip dimensions were 750  $\mu\text{m}$  x 220  $\mu\text{m}$ .

The highest light output power above 20mA injection current was achieved with 1.2%-In barriers (Figure 6) — at 70mA the increase over pure GaN barriers was 15.4%. The light output decreased significantly when the indium content in the barriers exceeded 2%.

Although the 2.0%-In barrier gave the highest peak external quantum efficiency (EQE), the 1.2%-In barrier was better at reducing the droop effect at higher injection current. At 70mA, the 2.0%- and 1.2%-In barriers gave EQE values 3.3% and 10.3% better than for pure GaN barriers, respectively.

The researchers therefore consider 1.2% indium to be the optimal content for InGaN barriers. X-ray analysis suggested that problems with increased indium content included increasing roughness of the well/barrier interface and degraded crystal quality.

One cause of such problems could be the increased lattice mismatch between the barrier and the underlying GaN lattice constant. The thinner wells should be less affected by crystal quality degradation,

despite the higher indium content. However, the reduced crystal quality of the barriers and the interface roughness do have their effect on the quality of subsequent well growth, inducing the creation of non-radiative recombination centers.

Photoluminescence analysis showed a slight reduction

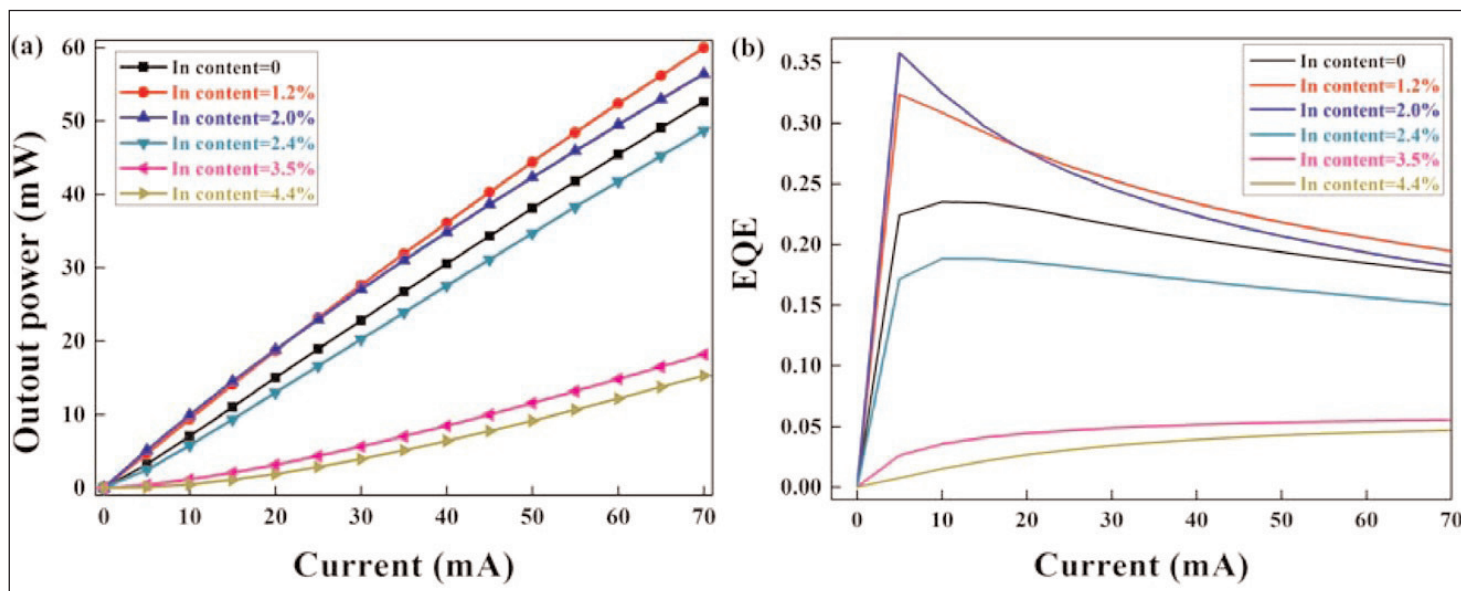


**Figure 6. (a) Light output power versus current and (b) EQE versus current.**

in intensity for 1.2%-In barriers, compared with pure GaN. As the indium content was increased beyond 1.2%, the photoluminescence decreased sharply.

The researchers used simulations to suggest that a positive effect of increasing indium content in the barriers was to increase carrier concentrations in the MQW structure. "We propose that the gain on carrier concentration and the crystalline quality degradation are a pair of opposite influential factors as the indium content of InGaN barriers increases," they write.

The calculations also suggest that the increase in indium increases the potential barrier for electrons while reducing that for holes.

### Ultraviolet light from ZnO

Jilin and Zhengzhou universities in China have increased the EL of zinc oxide/gallium nitride (ZnO/GaN) heterojunction light-emitting diodes (LEDs) by growing the crystal layers with oxygen/nitrogen polarities [Junyan Jiang et al, Appl. Phys. Lett., vol108, p063505, 2016].

The change from the more usual zinc/gallium polarity shifts the depletion layer of the p-n GaN-ZnO junction from the interface region into the ZnO, where recombination through excitons can lead to efficient production of ultraviolet (UV) photons. ZnO has a particularly strong  $\sim 60\text{meV}$  exciton binding of electron and holes. Also the direct bandgap is  $3.37\text{eV}$ .

The excitons in GaN have bindings around  $20\text{meV}$ , which is comparable to room temperature thermal effects ( $\sim 26\text{meV}$ ). ZnO p-n junctions are extremely difficult to realize because p-type material cannot be fabricated in a repeatable/reliable manner. There have been hopes of combining n-ZnO and p-GaN, but usually the EL is weak or undetectable from the ZnO side.

The LED materials were grown on c-plane sapphire ( $\text{Al}_2\text{O}_3$ ) substrates in an Aixtron CCS 3x2-inch flip-top MOCVD reactor.

The N-polar p-GaN layer had a hole concentration of  $2.4 \times 10^{17}/\text{cm}^3$ . The O-polar n-ZnO layer was produced in a two-step photo-assisted MOCVD process, using diethyl-zinc and oxygen precursors in argon carrier.

The two ZnO steps consisted of a  $450^\circ\text{C}/6\text{Torr}$  buffer,

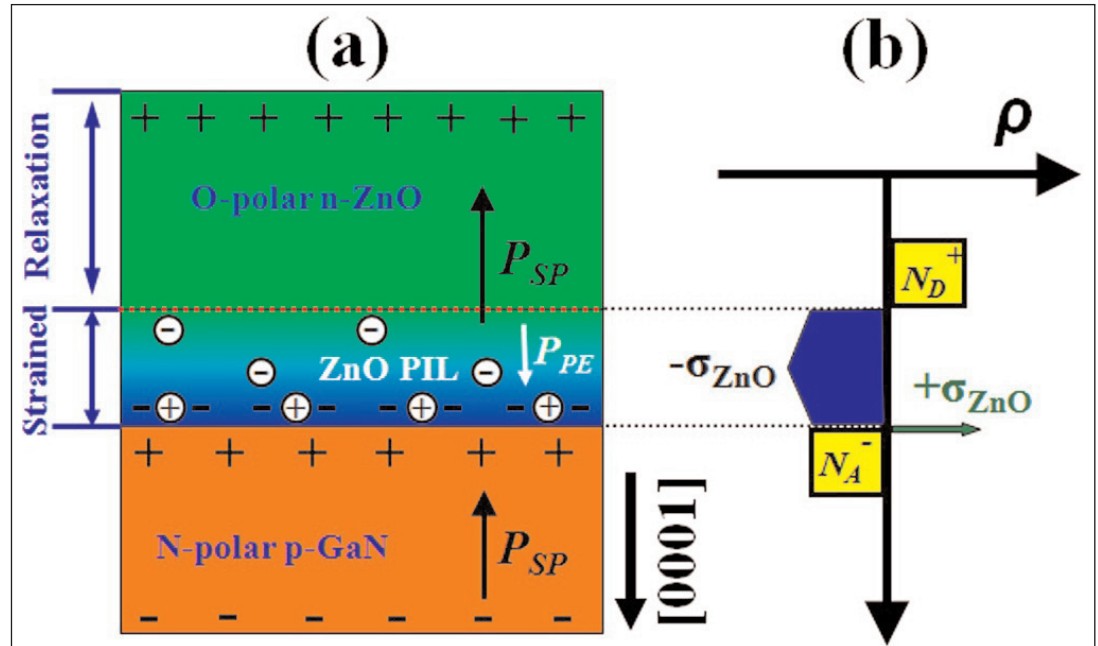


**Figure 7. (a) Schematic of O-polar n-ZnO/N-polar p-GaN heterostructure with polarization-induced inversion layer. Fixed charges induced by spontaneous and piezoelectric polarization are also displayed. (b) Spatial distribution of fixed polarization charges and ionized dopants in O-polar n-ZnO/N-polar p-GaN heterostructure.**

followed by a  $650^\circ\text{C}/12\text{Torr}$   $450\text{nm}$  layer. The electron concentration was  $2.7 \times 10^{17}/\text{cm}^3$ . Sputtered nickel/gold and gold were used as p-GaN and n-ZnO contacts for the LEDs.

Naively one expects the depletion region of a p-n junction to be mostly in the region with lowest carrier concentration. However, the chemical bonds of both ZnO and GaN have a large ionic component, resulting in charge polarization effects (Figure 7).

The different polarizations of ZnO and GaN give rise to charge dipole layers at interfaces and electric fields in the bulk of the material. There are both spontaneous and strain-dependent/piezoelectric polarization effects.

The early part of the ZnO layer is under compressive strain due to a 1.8% lattice mismatch with GaN. The compression relaxes later on in the growth. This leads to a polarization interface charge and a distributed charge from the varying strain as the ZnO relaxes.

In O-polar n-ZnO/N-polar p-GaN the depletion layer is shifted into the ZnO layer by a polarization-induced inversion layer (PIL). This gives rise to hopes that the electron-hole recombination will occur on the ZnO side, giving highly efficient UV emission based on excitons.

The LEDs had a turn-on voltage around  $3\text{V}$  and demonstrated rectifying behavior. The researchers observed "strong" UV EL centered at  $\sim 385\text{nm}$  (Figure 8). A Gaussian fit of the  $50\text{V}$  spectrum gave three peaks at  $383\text{nm}$ ,  $402\text{nm}$ , and  $430\text{nm}$ .

The researchers associated the strong  $383\text{nm}$  UV emission with ZnO near-band edge (NBE) transitions

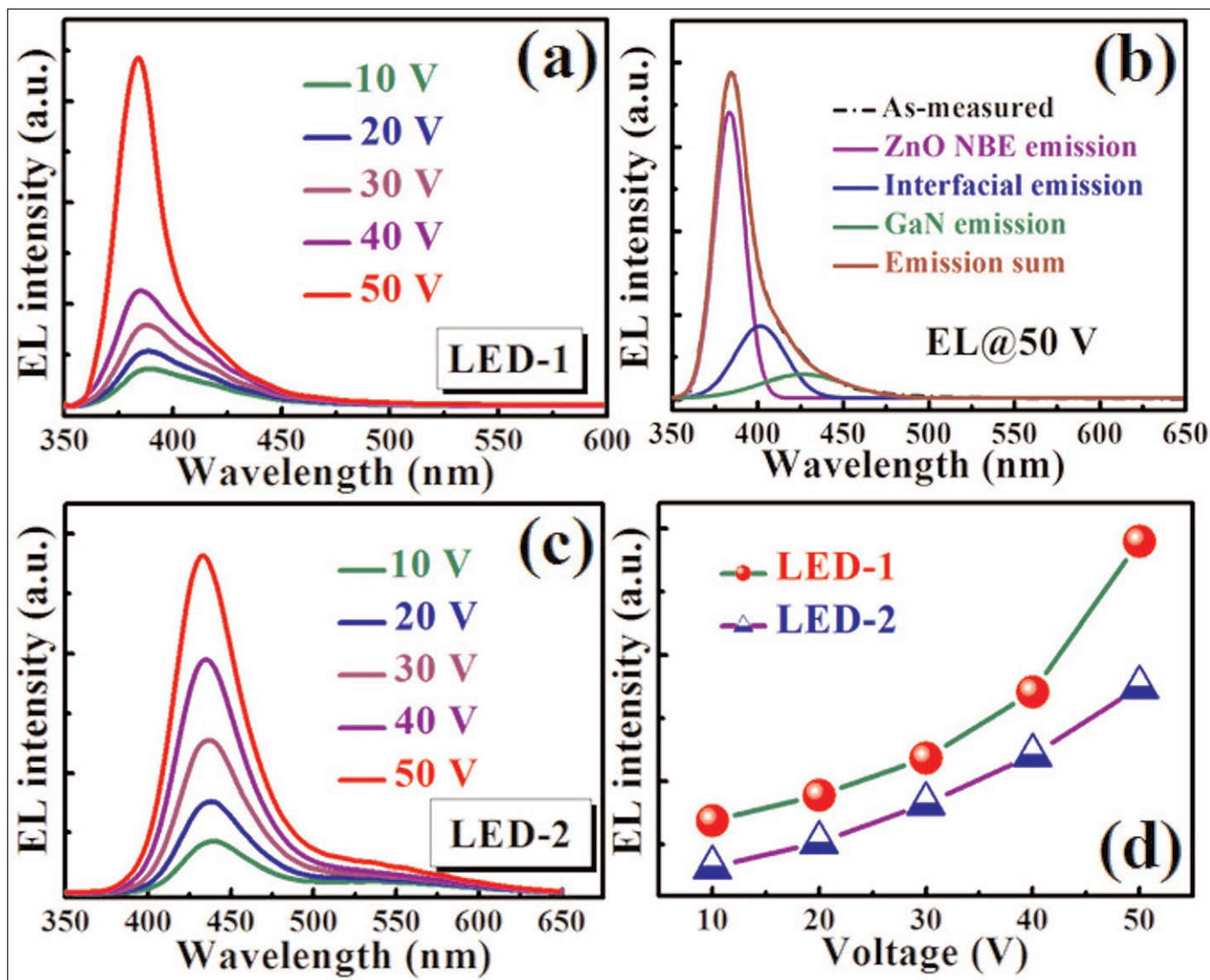


**Figure 8. (a) EL spectra of LED-1 (O-polar/N-polar) under various forward bias voltages ranging from 10V to 50V. (b) Gaussian deconvolution of a representative EL spectrum from LED-1 measured at 50V. (c) EL spectra of LED-2 (Zn-polar/Ga-polar) under various forward bias voltages ranging from 10V to 50V. (d) Relationship between integrated EL intensity and voltage of two LEDs.**

from free and bound excitons. The 430nm blue emission was attributed to transitions in the p-GaN to the magnesium acceptor level. The researchers add: "The blue emission at 402nm is from the interfacial recombination of the electrons from n-ZnO and the holes from p-GaN."

The researchers also produced a comparison LED-2 with Zn-polar n-ZnO and Ga-polar p-GaN. The p-GaN hole concentration was  $\sim 2 \times 10^{17}/\text{cm}^3$ . The EL emission from this device was broad and centered on 435nm (blue). The researchers interpret this as indicating that the depletion region is primarily on the p-GaN side. By contrast, the team believes the depletion region for the O-polar n-ZnO/N-polar p-GaN combination for LED-1 is completely on the ZnO side.

The group comments: "If the PIL of ZnO film is thick enough, the injected electrons and holes could be

effectively confined into ZnO side, producing UV emission from ZnO. More importantly, it is found that the light output power of LED-1 is relatively higher than that of LED-2 under the same test conditions."

At 50V, the O-polar n-ZnO/N-polar p-GaN LED-1 intensity exceeded that of LED-2 by 66%.

LED-1's full-width at half maximum became narrower with higher voltage: 48nm at 10V and 24nm at 50V. "As the forward bias changes from 10 to 50V, the intensity of ZnO NBE emission increases much faster than other two components. And it plays a dominant role when the forward bias is higher than 30V." The narrow NBE emission's increasing dominance reduces the FWHM value. ■

*The author Mike Cooke is a freelance technology journalist who has worked in the semiconductor and advanced technology sectors since 1997.*